

Original Research Paper

A Robust Medical Image Fusion Based on Synthetic Focusing Degree Criterion and Special Kernel Set for Clinical Diagnosis

¹Dawa Chyophel Lepcha, ¹Bhawna Goyal, ²Ayush Dogra, ³Ahmed Alkhayyat, ⁴Sanjeev Kumar Shah and ²Vinay Kukreja

¹Department of Electronics and Communication Engineering, Chandigarh University, Mohali, Punjab, India

²Chitkara University Institute of Engineering and Technology, Chitkara University, Punjab, India

³Department of Engineering, College of Technical Engineering, Islamic University, Najaf, Iraq

⁴Department of Electronics and Communication Engineering, Uttarakhand Institute of Technology, Uttarakhand University, Dehradun, India

Article history

Received: 07-08-2023

Revised: 26-12-2023

Accepted: 06-01-2024

Corresponding Author:

Ayush Dogra

Chitkara University Institute of Engineering and Technology, Chitkara University, Punjab, India

Email: ayush123456789@gmail.com

Abstract: Medical imaging has been widely used to diagnose diseases over the last two decades. Medical professionals still struggle to diagnose diseases using a single modality since there is a shortage of data in this domain. Therefore, images of specific organs with diseases from a variety of medical imaging systems can be combined using a technique called image fusion. Medical image fusion has prompted immense requisite applications in clinical applications in recent years. However, the fusion of medical images still facing a variety of challenges due to the input image quality. Protonema such as noise and low-contrast input medical images significantly reduces the quality of medical images. Still, recent image fusion methods are not significantly able to address the image quality problems. In order to address these problems, this study introduces a novel image fusion method that provides effective fusion performance even if the input images are noisy or low-contrast by combining the benefits of synthetic focusing degree criterion with a special kernel set. First, a Gaussian Curvature Filter (GCF) is used to sharpen the images in order to perform a Salient Feature Extraction (SFE). Then, we create a synthetic Focusing Degree Condition (FDC) that combines the Spatial Frequency (SF) and the Local Variance (LV) of the images to get the coarse fusion maps. The coarse fusion maps are then processed using median and morphological filters. The weighted fusion technology is used to generate the fused image. Finally, image enhancement is achieved by adding a special kernel to the fused image to obtain the final fusion result. Experimental results on the publicly available datasets exhibited that the proposed research article obtains the best results in terms of noisy and low-contrast medical images. Overall, it achieves significant performance both qualitatively and quantitatively when compared to other competing state-of-the-art methods.

Keywords: Medical Imaging, Image Fusion, Research, Gaussian Curvature Filter (GCF), Spatial Frequency, Technology

Introduction

Clinical diagnosis is significantly impacted by the quality of medical imaging. Consequently, increasing numbers of academics are focused on enhancing the performance of image fusion algorithms. These days, a

wide variety of medical images are utilized to diagnose diseases. As a matter of fact, in order to make a diagnosis, clinicians consult a wide range of image kinds for information. The reason for this is that single multimodal images do not provide adequate details appropriate for diagnosis purposes. For instance, radio frequency pulses

are used in Magnetic Resonance Imaging (MRI) to create images of the body's organs. It provides details such as fat tissue and muscular anatomy. In contrast, a CT scan is a diagnostic imaging method that generates images of the inside of the body by combining computer technology and X-rays. Any constituent of the body, including the bones, muscles, fat, organs and blood arteries is represented in great detail. A method called medical image synthesis adds extra data from multimodality medical images to produce a single which is a highly informative rich image (Haribabu *et al.*, 2023). Both the diagnosis process by physicians and the recognition of detecting devices will be more suitable with this technology. The transform domain-based image synthesis techniques are widely employed nowadays due to their effectiveness. The process of image fusion involves three main steps; (a) Transforming the image is the first stage. The objective of this stage is to help with the fusion by converting images into coefficients on the transform domain. The formation of synthetic images in a domain that has been changed by particular rules is the second phase. The max fusion principle (Li *et al.*, 2021a), an average fusion principle (Pei *et al.*, 2020), local gradient energy (Fu *et al.*, 2020) and MSMG-WLE (Zhang *et al.*, 2022) are a few examples of fusion principles that are introduced respectively. To generate a composite image, the elements generated through the transform domain are finally transferred to the spatial domain. Lepcha *et al.* (2020a) present a method to fuse medical images by using a cross-bilateral filter for gray-level similarities and geometric proximity of the neighboring pixels without smoothing borders. The rolling guiding filter is then used to filter the detailed images produced by deducting the cross bilateral filter image output from the original images in order to enable scale-aware operation. Many recent studies have employed image transformation techniques, including wavelet transform-based approaches (Tawfik *et al.*, 2021), Laplacian Decomposition (LD) (Li *et al.*, 2022) and Laplacian Pyramid (LP) transform (Fu *et al.*, 2020).

In addition, Goyal *et al.* presented a fusion technique that integrates poor-resolution medical photographs with a low computational period in order to enhance target detection accuracy and serve as a basis for clinical diagnosis (Goyal *et al.*, 2021). The Non-Subsampled Curvelet Transform (NSCT) (Li *et al.*, 2021b), contourlet transform (Yang *et al.*, 2010), Non-Subsampled Shearlet Transform (NSST) (Tannaz *et al.*, 2020) and curvelet transform (Nencini *et al.*, 2007) are few techniques that are based on multiscale geometric analysis. A novel technique for fusing multimodal medical images has been proposed recently (Goyal *et al.*, 2022). It uses edge-aware filtering and hybridization of cross-bilateral filters. This approach suggested a novel strategy for determining the

weights for the final fusion rule (Lilhore *et al.*, 2022; Ramesh *et al.*, 2022). In recent years, strategies for image synthesis based on sparse representation have also been presented. For instance, a novel approach to image synthesis based on Siamese networks and Sparse Representation (SR) was put forth by Yousif *et al.* (2022). In order to build an effective method for generating medical images, (Li *et al.*, 2021c) introduced fusion approach by combining SR method with a segment graph filter. The fusion method using pixel significance along with anisotropic diffusion and cross bilateral filtering is proposed by Lepcha *et al.* (2020b) This method initially methodology uses edge-preserving processing of input photographs with nonlinear techniques with a linear low pass filter to detect essential regions of source images while preserving edges. In order to identify the significant regions that are defined by edges of the right size and high amplitude, the morphological processing of linear filter residuals serves as the basis for the selection of those regions. Furthermore, a fusion method to fuse CT-SPECT images using discrete Hermite transform and SR was proposed by Barba-J *et al.* (2022). The traditional sparse representation (CSR) (Wang *et al.*, 2021a) and the Joint Sparse Model (JSM) (Zhang *et al.*, 2023a) are two examples of improvement strategies that are based on sparse representation.

In recent years, deep learning-based methods for medical image fusion have been proposed. For example, an image fusion technique that combines Convolutional Neural Network (CNN) and NSCT was presented by Wang *et al.* (2021b) The combination of SSN and the MSLES was proposed by Ding *et al.* (2021). The CNN was used and merged with SR by Shibu and Priyadharsini (2021). A cross-encoder (CE)-based technique for image synthesis was presented by Zhu *et al.* (2022) and Tawfik *et al.* (2022) introduced the usage of SAE in order to fuse medical photographs in the NSCT domain. An attention network called the Multi-scale Residual Pyramid (MRPAN) was proposed by Fu *et al.* (2020). Other deep learning-based techniques include multi-CNN, fuzzy neural networks (Fu *et al.*, 2020) and FusionNet (Xu and Ma, 2021). Furthermore, metaheuristic-related optimization methods have shown impressive medical image fusion efficiency in recent times. For instance, Duan *et al.* (2021) used SML in combination with a Genetic Algorithm (GA) and a log-Gabor filter. A method based on fuzzy logic and Particle Swarm Optimization (PSO) has been presented by Gao *et al.* (2021) The marine predator's algorithm (Dinh, 2023), equilibrium optimization algorithm (Dinh, 2021b), grasshopper optimization algorithm (Dinh, 2021a), gray wolf optimization (Daniel *et al.*, 2017) and PSO (Tannaz *et al.*, 2020) are a few further optimization methods that are currently in use. One recently proposed optimization

algorithm is the CSA (Braik, 2021). Many applications such as the diagnosis of plant leaf diseases (Umamageswari *et al.*, 2023), integrated heat and power economical dispatch (Rizk-Allah *et al.*, 2022), as well as feature selection (Mostafa *et al.*, 2022), have put together successful use of these algorithms. As a result, applying the CSA algorithm to image fusion and enhancement can yield inspiring results. The results indicate that a number of factors influence how well the image synthesis algorithm functions. The first is that there could be low-quality components in the input image, like noise or poor contrast. The majority of recent image fusion techniques are not able to handle input images with noise or poor contrast. Therefore, if there is an input image with poor image quality, the fusion performance of these methods is limited. Many recent researchers have also tried to preprocess the input photographs prior to the fusion of images. For instance, Maqsood and Javed (2020) Pre-processed the input image quality using an improved histogram equalization strategy.

The Fast Local Laplacian Filter (FLLF) was employed by Ullah *et al.* (2022) to enhance the quality of the source image in the image fusion method. For the fusion of medical images, (Zhang *et al.*, 2023b) provide a novel joint sparse model with coupled dictionary learning. In order to improve multi-source signal preservation and preserve edge/texture information, the framework designed a novel fusion rule. The standard sparse coefficients and novel sparse coefficients with overcomplete coupled dictionaries are used to represent the original medical images. Additionally, the authors developed a pair Feature Difference Guided Network (FDGNet), a novel end-to-end unsupervised learning fusion network for the fusion of medical images (Zhang *et al.*, 2023a). It is shown as feature-weighted guided learning in order for the image fusion task to effectively extract complementary properties from the input images. This means that the feature extraction method is responsible for determining the differences between properties at different stages and the feature restoring method could produce a pair of interactive weights by feature differences as guidance to produce fused results directly.

A novel end-to-end unsupervised network for fusing multi-modal medical images is presented by Liu *et al.* (2023) It consists of two symmetrical discriminators and a generator. Where the former seeks to create a "real-like" fused image based on precisely designed content and structural loss, whereas the latter is focused on identifying the differences between the fused image and the source ones. They receive alternating training until discriminators are unable to tell the fused image from the original one. Furthermore, preserving feature consistency across several modalities is facilitated by the symmetrical discriminator approach. However, the fused photographs' image quality has not been much better because these methods only slightly increase image quality. Thus, a

novel image fusion model is presented in this research that performs well even in cases where an input image has noise or poor contrast. The main contributions of the proposed method are as follows:

- 1) This study proposes a novel medical image fusion based on synthetic focusing degree criterion with a special kernel set to address the shortages of recent existing methods. To address this shortcoming, the proposed approach fully considers interrelated features between training sets and investigates relevant details between test images
- 2) An appropriate fusion approach that preserves functional and structural details is developed to highlight and enhance diverse information of source images
- 3) Experimental results illustrated that the proposed framework performs better in terms of both subjective visual evaluation and objective metrics and it is highly efficient when compared to the state-of-the-art fusion methods using publicly available datasets

Materials and Methods

This study introduces a novel medical image fusion based on synthetic focusing degree criterion with a special kernel set. This method applied a GCF-based technique where it produces the sharpest regions of the images. In addition, the feature images are obtained from the source images by subtracting the filtered images which provide edge information. Furthermore, the coarse fusion maps are generated using feature images and a synthetic FDC. The Optimized Fusion Maps (OFM) are obtained by the process of coarse fusion maps with morphological filters. The weighted fusion is used to generate the fused images. Lastly, a special kernel set is used to obtain the final fusion result while maintaining the significant details. Fig. 1 displays the framework of the proposed method.

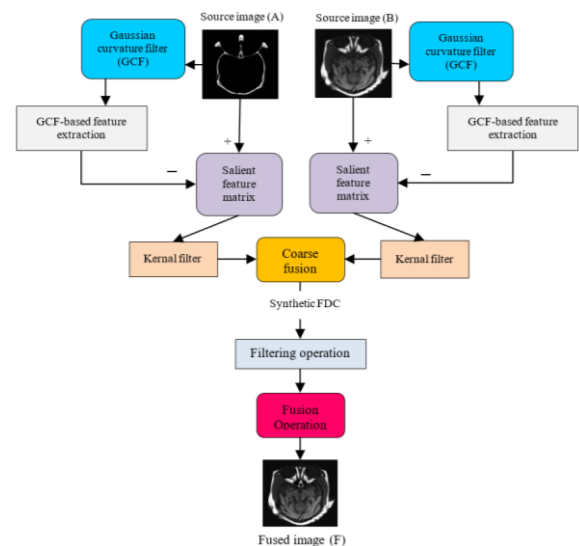


Fig. 1: Methodological flowchart of the proposed method

Salient Feature Extraction

The first step of our method is to extract edge features from the source images. The salient feature extraction procedure based on Gaussian Curvature Filter (GCF) is illustrated in this section.

Gaussian Curvature Filter (GCF)

An efficient image feature extraction technique that can synchronously safeguard the edges of images is introduced by Gong and Sbalzarini (2017). It assumed that the surface formed from a perfect, noise-free image is feasible and that the surface's Gaussian curvature is zero at any point. It is not necessary to explicitly calculate the Gaussian curvature by changing each pixel's value to align it with the tangent planes of nearby pixels. Therefore, second-order differentiability of surfaces is no longer necessary. The Gaussian filter for an image pixel located at (i, j) can be described as follows; the method first finds all the local tangent planes which include its neighborhood pixels to enumerate the pixel projections on the local surface:

$$d_1 = (U_{i-1,j} + U_{i+1,j})/2 - U_{i,j} \quad (1)$$

$$d_2 = (U_{i,j-1} + U_{i,j+1})/2 - U_{i,j}$$

$$d_3 = (U_{i-1,j-1} + U_{i+1,j+1})/2 - U_{i,j}$$

$$d_4 = (U_{i-1,j+1} + U_{i+1,j-1})/2 - U_{i,j}$$

$$d_5 = (U_{i-1,j} + U_{i,j-1} + U_{i-1,j-1})/3 - U_{i,j}$$

$$d_6 = (U_{i-1,j} + U_{i,j+1} + U_{i-1,j+1})/3 - U_{i,j}$$

$$d_7 = (U_{i,j-1} + U_{i+1,j} + U_{i+1,j-1})/3 - U_{i,j}$$

$$d_8 = (U_{i,j+1} + U_{i+1,j} + U_{i+1,j+1})/3 - U_{i,j}$$

where, d_n ($n = 1, 2, \dots, 8$) represents the distance between pixel (i, j) and the tangent planes of nearby pixels. Where $U_{i,j}$ stands for pixel value at location (i, j) . To find the closest local surface using the smallest projection distance as follows:

$$|d_m| = \min\{|d_n|, n = 1, 2, \dots, 8\} \quad (2)$$

In order to make pixel (i, j) fall on this surface, our method modifies its value as follows:

$$U'_{i,j} = U_{i,j} + d_m \quad (3)$$

where, $U'_{i,j}$ stands for pixel value at (i, j) . We utilize the sliding window approach to filter images from the top left to the bottom right to complete the filtering of the whole image. We can keep doing these adjustments until the

pixel values stop changing. For ease of use, the GCF operation is referred to in this study as GC (I, m) , where, I stands for input image and m stands for iterations number. The Salient Feature Extraction (SFE) from source images could be performed using the GCF.

GCF-Based Feature Extraction

The SFE from the source images could be performed using the GCF. The following is a description of the salient feature extraction process.

To obtain the filtered images, I_{GC1} and I_{GC2} , the GCF is employed for the source images I_1 and I_2 . The following is how the filtered images are obtained:

$$I_{GCn} = GC(I_n, m) \quad (n = 1, 2) \quad (4)$$

where, I_n and m represent the n^{th} source image and iterations number and $GC(\cdot)$ stands for the GCF operation.

The difference between filtered images and the source images is calculated to determine salient feature matrices. Therefore:

$$F_n = I_n - I_{GCn} \quad (5)$$

Focus Region Confirmation

Identification of the focus regions is significant in medical image fusion. Therefore, a suitable focus region validation process is required, where a synthetic FDC is proposed in our study. Where SF and LV constitute synthetic FDC. The coarse fusion map which could coarsely identify the focused and unfocused parts could be obtained using synthetic FDC.

Spatial Frequency

The entire process of image is represented by SF and the activity of image and clarity have a good relationship with the SF . Accordingly, if SF is high, an image will be clearer and its hierarchical structure will be clearer (Li *et al.*, 2001; Rahman *et al.*, 2017). In this study, a Row Frequency (RF) and Column Frequency (CF) are determined for a $P \times Q$ local patch in F_n that is centered at location (x, y) , where, P represents the row number and Q represents the number of the column:

$$RF_n(x, y) = \sqrt{\frac{1}{PQ} \sum_{x=1}^P \sum_{y=2}^Q [F_n(x, y) - F_n(x, y-1)]^2} \quad (6)$$

and:

$$CF_n(x, y) = \sqrt{\frac{1}{PQ} \sum_{x=1}^P \sum_{y=2}^Q [F_n(x, y) - F_n(x-1, y)]^2} \quad (7)$$

where the matrices for the salient features are F_1 and F_2 . Similarly, the SF can be described as:

$$SF_n(x, y) = \sqrt{RF_n(x, y)^2 + CF_n(x, y)^2} \quad (8)$$

Local Variance

The local map's clarity is measured using the *LV*. The *LV* can be used to effectively represent the detailed block. It reflects the contrast between minute details in images. Thus, we use *LV* as a local measure for finding regional priority regions. We have the following expression for $P \times Q$ local patch:

$$LV_n(x, y) = \sum_{r=-P/2}^{P/2} \sum_{s=-Q/2}^{Q/2} \frac{(F_n(x+r, y+s) - \mu_n)^2}{P \times Q} \quad (9)$$

where, μ_1 and μ_2 represent means of salient feature matrices F_1 and F_2 , respectively in local neighborhood $P \times Q$. Further, $P \times Q$ is fixed to 7×7 for complete experiments.

Focus Region Confirmation Using Synthetic FDC

We propose a synthetic FDC that combines *SF* and *LV*, where *SF* and *LV* describe complete qualities and local properties. By using this metric, we can produce coarse fusion maps that could represent both focused as well as unfocused parts. A coarse fusion map is represented by C_1 in this study as:

$$C_1(x, y) = \begin{cases} 1 & \text{if } SF_1(x, y) > SF_2(x, y) \text{ and} \\ & LV_1(x, y) > LV_2(x, y), \\ 0 & \text{otherwise} \end{cases} \quad (10)$$

It is clear that C_1 indicates regions of source image I_1 that were focused. In Eq. (10), "1" refers to the focussed regions of source image I_1 while "0" refers to the unfocused parts. The *SF* and *LV* are high in original images. The regions will only be categorised as focused regions if it is determined both measurements. Using a synthetic FDC makes a lot of sense because it considers both global and local details of the source images.

Filter Processing

Despite being able to approximate the focused and unfocused region distributions, the coarse fusion map generated from synthetic focus measure contains several thin flanges, slim fractures, slim gulfs and microscopic holes. Thus, more processing is required for coarse fusion maps. In this subsection, morphological filters and median filtering are utilized to fix these flaws. Thin connections and thin protrusions are no longer a concern due to the morphological opening operator. On the contrary, the morphological closing operator can combine narrow breaks and fill thin gaps as discussed in Rahman *et al.* (2017). The morphological filtering result for the coarse fusion map C_1 can be expressed as:

$$\begin{aligned} C_m &= (C_1 \ominus S) \oplus S, \\ C_n &= (C_1 \oplus S) \ominus S \end{aligned} \quad (11)$$

where, C_n is the map of the closure operation result and

C_m is the map of the opening process result. The terms \ominus and \oplus represents morphological dilation and erosion process, respectively in Eq. (11). S stands for an element of morphological structure with a radius size ranging from 2-15.

Image Fusion Process

If *OFM* is taken into consideration, the fused image I_F could be computed by:

$$I_F(i, j) = OFM(i, j) I_1(i, j) + (1 - OFM(i, j)) I_2(i, j) \quad (12)$$

Image Sharpening Using Special Kernel Set

It is relatively easy to Deblur images using kernels (Al-Ameen *et al.*, 2012). To generate a clearer image, we used the concept of convolving the kernel with the fused image. It only requires one mathematical process and is simple as well as accurate. Using the above Filtered Image (I_F), kernel (K) and convolution procedure (\otimes), the following procedure is defined for the restoring final fusion image (R):

$$R = I_F \otimes K \quad (13)$$

Results and Discussion

Datasets and Experimental Details

We considered nine pairs of medical images from the publicly available dataset (in Fig. 2) to validate the performance of the proposed method. A computer with a 2.6 GHz Intel Core i7 processor, 16 GB of RAM and an RTX2060 GPU was used for the experiments. All methods are implemented in MATLAB 2022b. For comparisons, we use seven algorithms, namely Laplacian pyramid and CNN reconstruction with local gradient energy strategy (LPCNNR) (Fu *et al.*, 2020), an unsupervised Enhanced Medical image fusion network (EM Fusion) (Xu and Ma, 2021), MRPAN (Fu *et al.*, 2021), a non-subsampled contourlet transform and CNN (NSCT-CNN) (Wang *et al.*, 2021a), a Cross Encoder Fusion (CEFusion) (Zhu *et al.*, 2022), FDGNet (Zhang *et al.*, 2023b) and Joint Sparse Model with Coupled Dictionary (JSM-CD) (Zhang *et al.*, 2023a) along with five metrics namely, Average Pixel Intensity (API) or mean (\bar{F}), Entropy (H), Average Gradient (AG), overall fusion efficiency (QAB/F) and information loss during fusion process ($L^{AB/F}$) (Goyal *et al.*, 2023) to evaluate techniques subjectively and objectively.

Fusion Quality Comparison of Medical Images

Fused results on CT1-MRI1 images. Figure 5 displays the qualitative fusion findings of three pairs of CT1 and MRI1 images. The fusion results of the first batch of CT1-MRI1 images from comparison techniques and our

approach are shown in Figs. 3(a-b1-10) displays the fused images of the second batch of CT1-MRI1 images on all approaches. The final set of sources, including CT1-MRI1 images and the fused images of all techniques are presented in Fig. 3(c1-10). Soft tissue structure is not well reproduced by MRPAN or EMFusion. The low brightness of results is caused by CT1 information loss in LPCNNR and CEFusion. Rich texture details are not obtained via FDGNet and CEFusion. Functional information on NSCT-CNN is absent. The fusion results of FDGNet and JSM-CD show distorted MRI image information. It is simple to observe visually that our algorithm preserves both structural and functional information (soft tissue, skull). This is evident when comparing the results of all approaches. The clearest details can be found in the fused images. This suggests that our technique produces fusion results with the highest level of image detail preservation.

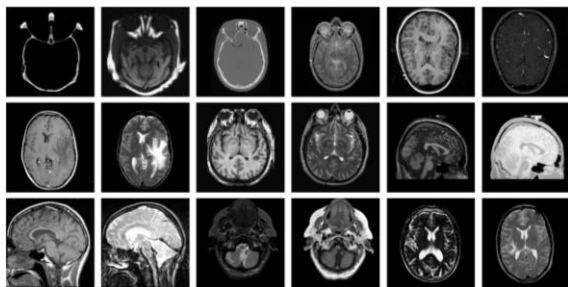


Fig. 2: 9 pairs of medical images (CT/MR) used in the experiments

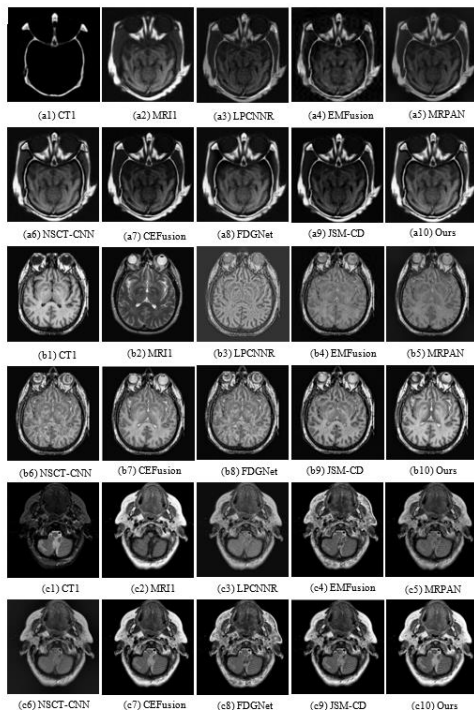


Fig. 3: Fusion examples for 'CT1-MR1' image

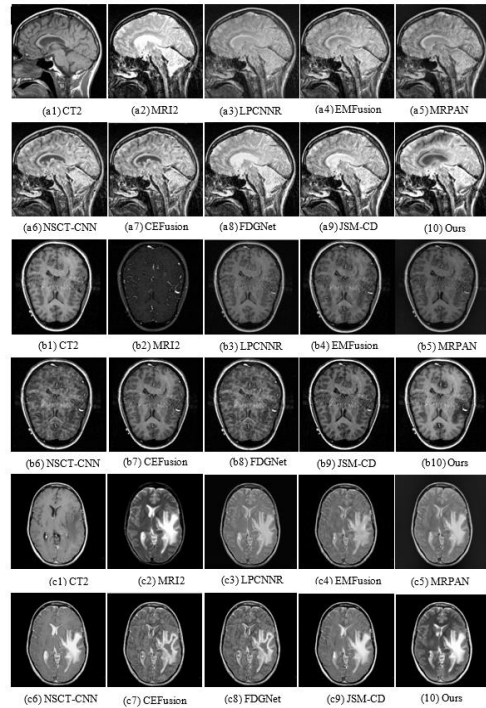


Fig. 4: Fusion examples for 'CT2-MR2' image

Fused results on CT2/MRI2 images. Three pairs of fusion results, viz CT2 and MRI2 imaging data are presented in Fig. 4. The first two rows display the results on the initial batch of CT2/MRI2 images using all methods, similar to Fig. 3. The second set of CT2/MRI2 fused results are shown in the center two rows. The final two rows list the findings from the third batch of CT2/MRI2 scans. EMFusion produces poor fused results because it loses CT features (caudate body). In MRI2 images, highlighted information (such as the caudate body) is distorted by LPCNNR. The dense structure of CT source images is weakened by CEFusion. The results of FDGNet and CEFusion are hazy. While performing better than the previously mentioned techniques, NSCT-CNN, MRPAN, FDGNet and JSM-CD still could not match our approach which maintains dense soft tissue structure while preserving edge details. Two benefits of our strategy are shown by an analysis of Fig. 4. Firstly, reduced brightness in CT images is compensated for by high-quality details in MRI scans. Second, significant information from the original images is maintained in the fused results simultaneously.

Fused results on other pairs of medical images. The fused images from the additional three medical image pairs are performed experimentally. Our approach was able to transfer more features from input images to the final fusion images by combining the analysis of Figs. 3-4. By carefully observing the image pair results, this subjective result validates that the proposed fusion rule can preserve the maximum extent of source image information.

Table 1: Mean quantitative metrics of medical images (Fig. 2) using different techniques (Red+ (1), violet + (2) and green + (3) are the first, second and third scores, respectively)

	LPCNNR [4]	EMFusion [29]	MRPAN [28]	NSCT-CNN [23]	CEFusion [26]	FDGNet [42]	JSM-CD [22]	Ours
API	33.67730	35.88270	38.88270	44.99220	49.88160	53.98920	52.9971	55.9927
H	4.27720	4.67150	5.21550	5.75250	6.01650	6.34410	6.8016	7.2315
AG	6.77260	7.21770	7.78180	8.78810	9.78442	9.75160	9.7521	11.9971
$Q^{AB/F}$	0.76240	0.79250	0.81770	0.83550	0.86550	0.88150	0.8976	0.9014
$L^{AB/F}$	0.27730	0.21980	0.18820	0.15260	0.12770	0.10230	0.0981	0.0871

Table 2: Average time consumption of all techniques for fusion of medical images (unit: s)

LPCNNR [4]	EMFusion [29]	MRPAN [28]	NSCT-CNN [23]	CEFusion [26]	FDGNet [42]	JSM-CD [22]	Our
38.3	15.9	23.8	40.6	18.5	56.8	34.7	8.6

Objectives Evaluation for Medical Images

The mean value of the quantitative evaluation for all algorithms on medical images (Fig. 2) is tabulated in Table 1. Table 1 clearly shows that AG, entropy (H), API, $Q^{AB/F}$ and $L^{AB/F}$ are the highest in the case of the proposed method as compared to other competing methods. The higher AG values show that the results of the proposed method effectively preserve the functional and structural information present in the original images. The best $Q^{AB/F}$ results demonstrate the contrast-optimal nature of our approach. It illustrates how fused results are less prone to noise and have more texture and detail. The less $L^{AB/F}$ suggests the proposed method performance avoids distortion and is comparable to the standard images. Based on an analysis and observation of Table 1, it can be concluded that our method is capable of preserving both functional and structural details due to the ideal values for measurements. As a result, the subjective analysis and objective evaluation coincide with providing more proof that our approach produces the best results.

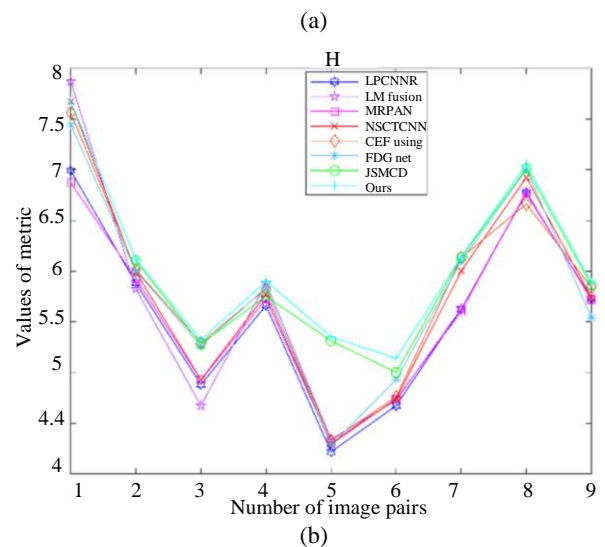
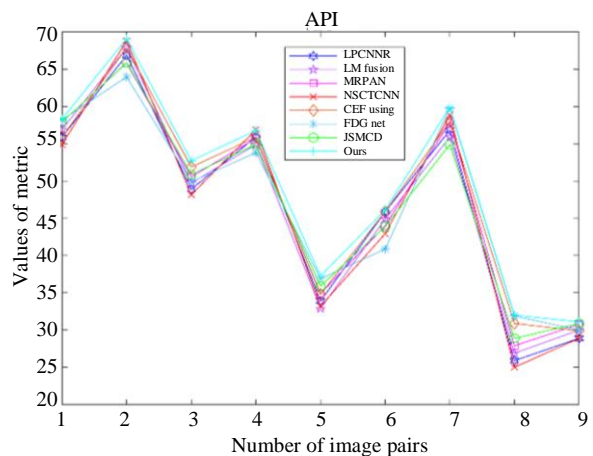
Further Objective Graphical Representations

The objective analysis of different image fusion techniques is presented in Table 1. The objective assessment metric values for 9 image sets are presented in Fig. 5. to further illustrate the efficiency of our strategy. When examining Fig. 5, it is clear that our approach performs best on all objective metrics such as AG, H, API $Q^{AB/F}$ and $L^{AB/F}$ for every pair of images. These conclusions indicate that our method preserves better functional and structural details from the original images in the fused results. The proposed method of fused image contrast is cleaner and more consistent with visual perception when compared to the comparative methods.

Operating Efficiency of All Fusion Algorithms

Table 2 presents the mean time spent on nine pairs of 256×256 CT/MRI images utilizing Table 2: Average time consumption of all techniques for fusion of medical images (unit: s) proposed method in addition to seven state-of-the-art methods. Based on an intuitive

observation of Table 2, our solution outperforms other methods and is placed in first place requiring a less time-consuming kernel set to enhance input images. By using a synthetic focusing degree criterion, the proposed solution greatly lowers the time cost as compared to other methods. Our approach outperforms other algorithms in the case of both qualitative and quantitative analysis but marginally improves in some cases.



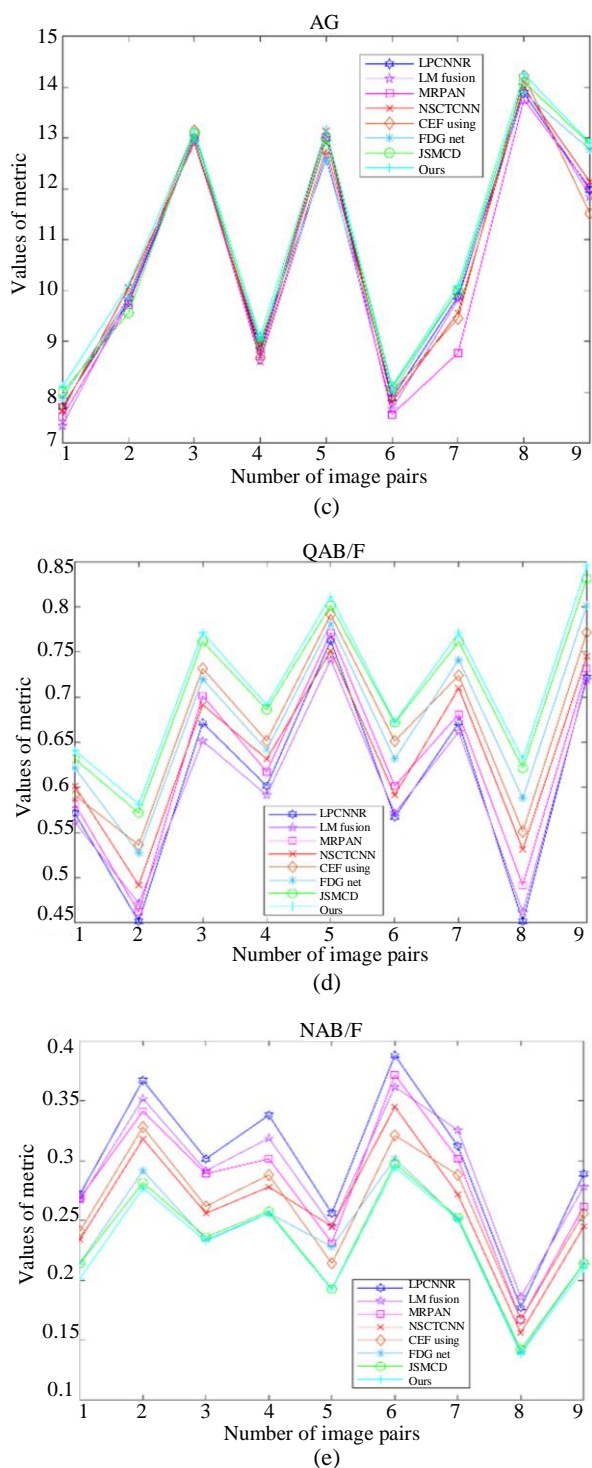


Fig. 5: Comparison of 9 pairs of CT/MRI images on fusion algorithms by using different metrics: (a) API; (b) Entropy (H); (c) AG; (d) $Q^{AB/F}$; (e) $L^{AB/F}$

Conclusion

In this study, a synthetic focusing degree criterion with a special kernel set is used for medical image fusion to

achieve the best fusion performance. Firstly, the GCF is used to get the sharpest parts of the medical images by carrying out salient feature extraction. Then, we generate a synthetic FDC that combines the SF and LV of the image to obtain the coarse fusion maps. To generate optimized fusion maps, the course fusion maps are further processed using median and morphological filters. A weight fusion process is utilized to obtain fused images. The enhancement is then accomplished by adding a specific kernel set to the fused images. The proposed algorithm validates capability using nine pairs of CT-MRI medical images.

The proposed approach decreases computational complexity and execution time while improving diagnostic computing accuracy. Our method exhibits a major boost in competence when compared to other competing algorithms. It can be observed that the qualitative interpretation of all the fused images recovered through the proposed algorithm has superior visual quality. However, this method is not able to work for different types of medical images which is its limitations. Our method can be upgraded by using different types of filters which have been left for future research works. Furthermore, image fusion and the importance of this technique have huge prospects for improvement by proposing several image fusion algorithms in order to reduce noise and artifacts.

Acknowledgment

We would like to thank all persons had contributed to this study. Also, we express our gratitude to the study's reviewers and editors.

Funding Information

This study did not receive funds from either public or private entities.

Author's Contributions

All authors equally contributed in this study.

Ethics

The corresponding authors declared that this study has not been submitted elsewhere. Also, the authors declared no conflict of interest.

References

- Al-Ameen, Z., Sulong, G., & Johar, M. G. M. (2012). Fast deblurring method for computed tomography medical images using a novel kernels set. *International Journal of Bio-Science and Bio-Technology*, 4(3), 9-20.
https://gvpress.com/journals/IJBSBT/vol4_no3/2.pdf

- Barba-J, L., Vargas-Quintero, L., & Calderón-Agudelo, J. A. (2022). Bone SPECT/CT image fusion based on the discrete hermite transform and sparse representation. *Biomedical Signal Processing and Control*, 71, 103096.
<https://doi.org/10.1016/J.BSPC.2021.103096>
- Braik, M. S. (2021). Chameleon Swarm Algorithm: A bio-inspired optimizer for solving engineering design problems. *Expert Systems with Applications*, 174, 114685.
<https://doi.org/10.1016/J.ESWA.2021.114685>
- Daniel, E., Anitha, J., Kamaleshwaran, K. K., & Rani, I. (2017). Optimum spectrum mask based medical image fusion using Gray Wolf Optimization. *Biomedical Signal Processing and Control*, 34, 36-43.
<https://doi.org/10.1016/J.BSPC.2017.01.003>
- Ding, Z., Zhou, D., Li, H., Hou, R., & Liu, Y. (2021). Siamese networks and multi-scale local extrema scheme for multimodal brain medical image fusion. *Biomedical Signal Processing and Control*, 68, 102697.
<https://doi.org/10.1016/J.BSPC.2021.102697>
- Dinh, P. H. (2021a). A novel approach based on grasshopper optimization algorithm for medical image fusion. *Expert Systems with Applications*, 171, 114576.
<https://doi.org/10.1016/J.ESWA.2021.114576>
- Dinh, P. H. (2021b). Combining gabor energy with equilibrium optimizer algorithm for multi-modality medical image fusion. *Biomedical Signal Processing and Control*, 68, 102696.
<https://doi.org/10.1016/J.BSPC.2021.102696>
- Dinh, P. H. (2023). A novel approach based on marine predators algorithm for medical image enhancement. *Sensing and Imaging*, 24(1), 6.
<https://doi.org/10.1007/S11220-023-00411-Y/METRICS>
- Duan, J., Mao, S., Jin, J., Zhou, Z., Chen, L., & Chen, C. P. (2021). A novel GA-based optimized approach for regional multimodal medical image fusion with superpixel segmentation. *IEEE Access*, 9, 96353-96366.
<https://doi.org/10.1109/ACCESS.2021.3094972>
- Fu, J., Li, W., Du, J., & Huang, Y. (2021). A multiscale residual pyramid attention network for medical image fusion. *Biomedical Signal Processing and Control*, 66, 102488.
<https://doi.org/10.1016/J.BSPC.2021.102488>
- Fu, J., Li, W., Du, J., & Xiao, B. (2020). Multimodal medical image fusion via laplacian pyramid and convolutional neural network reconstruction with local gradient energy strategy. *Computers in Biology and Medicine*, 126, 104048.
<https://doi.org/10.1016/J.COMPBIOMED.2020.104048>
- Gao, Y., Ma, S., Liu, J., Liu, Y., & Zhang, X. (2021). Fusion of medical images based on salient features extraction by PSO optimized fuzzy logic in NSST domain. *Biomedical Signal Processing and Control*, 69, 102852.
<https://doi.org/10.1016/J.BSPC.2021.102852>
- Gong, Y., & Sbalzarini, I. F. (2017). Curvature filters efficiently reduce certain variational energies. *IEEE Transactions on Image Processing*, 26(4), 1786-1798.
<https://doi.org/10.1109/TIP.2017.2658954>
- Goyal, B., Lepcha, D. C., Dogra, A., Bhateja, V., & Lay-Ekuakille, A. (2021). Measurement and analysis of multi-modal image fusion metrics based on structure awareness using domain transform filtering. *Measurement*, 182, 109663.
<https://doi.org/10.1016/J.MEASUREMENT.2021.109663>
- Goyal, B., Dogra, A., Lepcha, D. C., Koundal, D., Alhudaif, A., Alenezi, F., & Althubiti, S. A. (2022). Multi-modality image fusion for medical assistive technology management based on hybrid domain filtering. *Expert Systems with Applications*, 209, 118283.
<https://doi.org/10.1016/J.ESWA.2022.118283>
- Goyal, B., Dogra, A., Khoond, R., Lepcha, D. C., Goyal, V., & Fernandes, S. L. (2023). Medical Image Fusion Based on Anisotropic Diffusion and Non-Subsampled Contourlet Transform. *Computers, Materials and Continua*, 76(1).
<https://doi.org/10.32604/CMC.2023.038398>
- Haribabu, M., Guruviah, V., & Yogarajah, P. (2023). Recent Advancements in Multimodal Medical Image Fusion Techniques for Better Diagnosis: An overview. *Current Medical Imaging*, 19(7), 673-694.
<https://doi.org/10.2174/1573405618666220606161137>
- Lepcha, D. C., Dogra, A., Goyal, B., Chohan, J. S., Koundal, D., Zaguia, A., & Hamam, H. (2022a). Multimodal medical image fusion based on pixel significance using anisotropic diffusion and cross bilateral filter. *Hum.-Cent. Comput. Inf. Sci*, 12.
<https://doi.org/10.22967/HGIS.2022.12.015>
- Lepcha, D. C., Goyal, B., & Dogra, A. (2020b). Image fusion based on cross bilateral and rolling guidance filter through weight normalization. *The Open Neuroimaging Journal*, 13(1).
<https://doi.org/10.2174/1874440002013010051>
- Li, S., Kwok, J. T., & Wang, Y. (2001). Combination of images with diverse focuses using the spatial frequency. *Information Fusion*, 2(3), 169-176.
[https://doi.org/10.1016/S1566-2535\(01\)00038-0](https://doi.org/10.1016/S1566-2535(01)00038-0)
- Li, Q., Wang, W., Chen, G., & Zhao, D. (2021a). Medical image fusion using segment graph filter and sparse representation. *Computers in Biology and Medicine*, 131, 104239.
<https://doi.org/10.1016/J.COMPBIOMED.2021.104239>

- Li, W., Lin, Q., Wang, K., & Cai, K. (2021b). Improving medical image fusion method using fuzzy entropy and non-subsampling contourlet transform. *International Journal of Imaging Systems and Technology*, 31(1), 204-214. <https://doi.org/10.1002/IMA.22476>
- Li, X., Zhou, F., Tan, H., Zhang, W., & Zhao, C. (2021c). Multimodal medical image fusion based on joint bilateral filter and local gradient energy. *Information Sciences*, 569, 302-325. <https://doi.org/10.1016/J.INS.2021.04.052>
- Li, W., Chao, F., Wang, G., Fu, J., & Peng, X. (2022). Medical image fusion based on local Laplacian decomposition and iterative joint filter. *International Journal of Imaging Systems and Technology*, 32(5), 1631-1645. <https://doi.org/10.1002/IMA.22714>
- Lilhore, U. K., Poongodi, M., Kaur, A., Simaiya, S., Algarni, A. D., Elmannai, H., ... & Hamdi, M. (2022). Hybrid model for detection of cervical cancer using causal analysis and machine learning techniques. *Computational and Mathematical Methods in Medicine*, 2022. <https://doi.org/10.1155/2022/4688327>
- Liu, H., Li, S., Zhu, J., Deng, K., Liu, M., & Nie, L. (2023). DDIFN: A Dual-discriminator Multi-modal Medical Image Fusion Network. *ACM Transactions on Multimedia Computing, Communications and Applications*, 19(4), 1-17. <https://doi.org/10.1145/3574136>
- Maqsood, S., & Javed, U. (2020). Multi-modal medical image fusion based on two-scale image decomposition and sparse representation. *Biomedical Signal Processing and Control*, 57, 101810. <https://doi.org/10.1016/J.BSPC.2019.101810>
- Mostafa, R. R., Ewees, A. A., Ghoniem, R. M., Abualigah, L., & Hashim, F. A. (2022). Boosting chameleon swarm algorithm with consumption AEO operator for global optimization and feature selection. *Knowledge-Based Systems*, 246, 108743. <https://doi.org/10.1016/J.KNOSYS.2022.108743>
- Nencini, F., Garzelli, A., Baronti, S., & Alparone, L. (2007). Remote sensing image fusion using the curvelet transform. *Information Fusion*, 8(2), 143-156. <https://doi.org/10.1016/J.INFFUS.2006.02.001>
- Pei, C., Fan, K., & Wang, W. (2020). Two-scale multimodal medical image fusion based on guided filtering and sparse representation. *IEEE Access*, 8, 140216-140233. <https://doi.org/10.1109/ACCESS.2020.3013027>
- Rahman, M. A., Liu, S., Wong, C. Y., Lin, S. C. F., Liu, S. C., & Kwok, N. M. (2017). Multi-focal image fusion using degree of focus and fuzzy logic. *Digital Signal Processing*, 60, 1-19. <https://doi.org/10.1016/J.DSP.2016.08.004>
- Ramesh, T. R., Lilhore, U. K., Poongodi, M., Simaiya, S., Kaur, A., & Hamdi, M. (2022). Predictive analysis of heart diseases with machine learning approaches. *Malaysian Journal of Computer Science*, 132-148. <https://doi.org/10.22452/MJCS.SP2022NO1.10>
- Rizk-Allah, R. M., Hassanien, A. E., & Snášel, V. (2022). A hybrid chameleon swarm algorithm with superiority of feasible solutions for optimal combined heat and power economic dispatch problem. *Energy*, 254, 124340. <https://doi.org/10.1016/J.ENERGY.2022.124340>
- Yousif, A. S., Omar, Z., & Sheikh, U. U. (2022). An improved approach for medical image fusion using sparse representation and Siamese convolutional neural network. *Biomedical Signal Processing and Control*, 72, 103357. <https://doi.org/10.1016/J.BSPC.2021.103357>
- Shibu, D. S., & Priyadharsini, S. S. (2021). Multi scale decomposition based medical image fusion using convolutional neural network and sparse representation. *Biomedical Signal Processing and Control*, 69, 102789. <https://doi.org/10.1016/J.BSPC.2021.102789>
- Tannaz, A., Mousa, S., Sabalan, D., & Masoud, P. (2020). Fusion of multimodal medical images using nonsubsampling shearlet transform and particle swarm optimization. *Multidimensional Systems and Signal Processing*, 31, 269-287. <https://doi.org/10.1007/s11045-019-00662-7>
- Tawfik, N., Elnemr, H. A., Fakh, M., Dessouky, M. I., & Abd El-Samie, F. E. (2021). Hybrid pixel-feature fusion system for multimodal medical images. *Journal of Ambient Intelligence and Humanized Computing*, 12(6), 6001-6018. <https://doi.org/10.1007/s12652-020-02154-0>
- Tawfik, N., Elnemr, H. A., Fakh, M., Dessouky, M. I., & El-Samie, F. E. A. (2022). Multimodal medical image fusion using stacked auto-encoder in NSCT domain. *Journal of Digital Imaging*, 35(5), 1308-1325. <https://doi.org/10.1007/s10278-021-00554-y>
- Ullah, H., Zhao, Y., Abdalla, F. Y., & Wu, L. (2022). Fast local Laplacian filtering based enhanced medical image fusion using parameter-adaptive PCNN and local features-based fuzzy weighted matrices. *Applied Intelligence*, 1-20. <https://doi.org/10.1007/s10489-021-02834-0>
- Umamageswari, A., Bharathiraja, N., & Irene, D. S. (2023). A novel fuzzy C-means based chameleon swarm algorithm for segmentation and progressive neural architecture search for plant disease classification. *ICT Express*, 9(2), 160-167. <https://doi.org/10.1016/J.ICTE.2021.08.019>

- Wang, L., Dou, J., Qin, P., Lin, S., Gao, Y., Wang, R., & Zhang, J. (2021a). Multimodal medical image fusion based on nonsubsampling shearlet transform and convolutional sparse representation. *Multimedia Tools and Applications*, 80, 36401-36421. <https://doi.org/10.1007/s11042-021-11379-w>
- Wang, Z., Li, X., Duan, H., Su, Y., Zhang, X., & Guan, X. (2021b). Medical image fusion based on convolutional neural networks and non-subsampling contourlet transform. *Expert Systems with Applications*, 171, 114574. <https://doi.org/10.1016/J.ESWA.2021.114574>
- Xu, H., & Ma, J. (2021). EMFusion: An unsupervised enhanced medical image fusion network. *Information Fusion*, 76, 177-186. <https://doi.org/10.1016/J.INFFUS.2021.06.001>
- Yang, S., Wang, M., Jiao, L., Wu, R., & Wang, Z. (2010). Image fusion based on a new contourlet packet. *Information Fusion*, 11(2), 78-84. <https://doi.org/10.1016/J.INFFUS.2009.05.001>
- Zhang, C., Zhang, Z., Feng, Z., & Yi, L. (2023a). Joint sparse model with coupled dictionary for medical image fusion. *Biomedical Signal Processing and Control*, 79, 104030. <https://doi.org/10.1016/J.BSPC.2022.104030>
- Zhang, G., Nie, R., Cao, J., Chen, L., & Zhu, Y. (2023b). FDGNet: A pair feature difference guided network for multimodal medical image fusion. *Biomedical Signal Processing and Control*, 81, 104545. <https://doi.org/10.1016/J.BSPC.2022.104545>
- Zhang, Y., Jin, M., & Huang, G. (2022). Medical image fusion based on improved multi-scale morphology gradient-weighted local energy and visual saliency map. *Biomedical Signal Processing and Control*, 74, 103535. <https://doi.org/10.1016/J.BSPC.2022.103535>
- Zhu, Y., Wang, X., Chen, L., & Nie, R. (2022). CEFusion: Multi-Modal medical image fusion via cross encoder. *IET Image Processing*, 16(12), 3177-3189. <https://doi.org/10.1049/IPR2.12549>